Variations in Mass Flow Rate and Number of Channels in The Prismatic Form Lithium-Ion Battery Cell Cooling System Using Water Cooling and Ethylene Glycol By Computational Fluid Dynamics (CFD) Method

Byan Wahyu Riyandwita[1,*], Sylvia Ayu Pradanawati[2], Mohammad Nazri[3]

{byan.wr@universitaspertamina.ac.id[1], sylvia.pradanawati@universitaspertamina.ac.id[2], nazrinaning@gmail.com[3]}

Department of Mechanical Engineering, Faculty of Industrial Technology, Universitas Pertamina, Indonesia[1,2,3]

Abstract. Battery thermal management is an important aspect of battery life. This research delves into the use of a cooling system for lithium-ion batteries specifically employing a channel plate with different configurations of channels and two types of cooling fluids water and ethylene glycol. The fluid dynamic (CFD) method is utilized to analyze the cooling performance. The main objective is to examine how effectively water and ethylene glycol can maintain the battery temperature below its operating threshold using the mini channel plate design. Although there is a slight impact on cooling, increasing the number of channels has a significant effect of a 25% reduction in pressure drop. Furthermore, enhancing the inlet mass flow rate of both water and ethylene glycol cooling fluids results in improved cooling capability. It is also observed from the result that ethylene glycol outperforms water in terms of cooling performance.

Keywords: Lithium-ion battery, Cooling, Ethylene glycol, Computational fluid dynamics

1 Introduction

Indonesia is considered to be one of the developing nations, with a large population. It is quite common for Indonesians to rely on motorized vehicles for their transportation needs. According to data provided by the Central Statistics Agency (BPS) in 2020 there were 138.13 million fossil fuel based motor vehicles in Indonesia [1]. The widespread use of vehicles powered by fossil fuels not only contributes to the problem of limited fossil energy resources but also leads to emissions issues both within Indonesia and globally. To address these challenges automobile manufacturers have initiated a transition towards energy alternatives like electric car. As a testament to Indonesias commitment towards energy transition, Presidential Regulation (Perpres) Number 55 of 2019 was introduced focusing on expediting the adoption of battery powered electric motor vehicles, for road transportation purposes.

ICO-SEID 2022, November 23-24, Jakarta, Indonesia

DOI 10.4108/eai.23-11-2022.2341544

Electric motorized vehicles that use batteries are usually referred to as Battery Electrical Vehicles (BEV). It is a type of electric vehicle that utilizes batteries as storage of electrical energy which will later be converted into mechanical energy by electric motors. The electrical energy will be stored in the battery which is an electronic component. A battery consists of electrochemical cells allowing it to generate and provide energy. The type of battery commonly used is the lithium-ion type.

Lithium-ion batteries would be the batteries with the highest manufacturing demand, amounting to nearly 660 million cells annually [2]. Lithium ion batteries are commonly preferred due to their ability to store a high amount of energy, compact size and minimal loss of discharge over time [3-5]. Table 1 shows some of the capabilities possessed by lithium-ion batteries that make lithium-ion batteries much better compared to other types of batteries.

Table 1. Common Rechargeable Batteries Characteristics [5].

Property	**NiCd**	**NiMH**	**Lead Acid**	**Li-ion**	**Li-ion polymer**	**AGM VRSLAB**
Gravimetric energy density (Wh/kg)	45-80	60-120	30-50	100-200	150-250	>100
Internal resistance (mΩ)	100-200 (12V pack)	200-300 (6V pack)	<100 (12V pack)	150-250 (7.2V pack)	200-300 (7.2V pack)	<50 (12V pack)
80% life cycle (cycles)	1,500	500	300	1,000	500	3,000
Fast charge time	1h typical	2-4h	8-16h	2-4h	2-4h	<1h
Overcharge tolerance	moderate	low	high	very low	low	very high
Charge/discharge efficiency (%)	70-90%	66%	50-92%	80-90%	>90%	98%
Self discharge/month	20%	30%	5%	10%	~10%	1-3%
Nominal cell voltage	1.25V	1.25V	2V	3.6V	3.6V	2V
Load current (peak/rated) (%)	2,000	500	500	>200	>200	>2,000
Discharge operating temperature	-40-60°C	-20-60°C	-20-60°C	-20-60°C	0-60°C	-40-60°C
Maintenance requirement	60 days	60-90 days	3-6 months	not req.	not req.	not req.
Typical battery cost (USD)	$100 (7.2V)	$60 (7.2V)	$25 (12V)	$100 (7.2V)	$100 (7.2V)	$100 (12V)
Cost/life cycle ($/cycles)	$0.08	$0.12	$0.1	$0.1	$0.29	$0.03-0.04
Commercial used since	1950	1990	1970	1991	1999	1985

Based on the cell geometry, the lithium-ion battery has a cylinder and prismatic shape, whereas the prismatic shape consists of prismatic hard-case cells and the prismatic pouch cell shapes based on their housing stability. The advantage of a battery with a prismatic shape is that it can provide a very large voltage capacity and the case owned by prismatic geometry is stronger than other shapes so that many once its application is mainly for electric car vehicles. On average the pouch cell weighs 20% less than the hard case cell. It has a capacity that is nearly 50% higher, at the same volume [6].

In addition, lithium-ion batteries also have disadvantages, one of which is that they are very sensitive to temperature [7]. Even though it is suggested that the acceptable temperature range for operating a lithium ion battery during discharge is 20 to 60°C [5], it is preferable to keep the battery within the range of 15 to 35°C. This is because excessive heat can have effects on the batterys performance, safety and overall lifespan [8]. **Figure 1** illustrates how the operating temperature directly impacts the performance of lithium ion batteries. Thus it becomes crucial to have a thermal management system in place to maintain the batterys temperature.

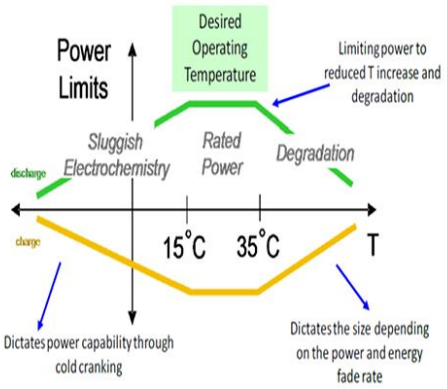

Fig. 1. Performance map of lithium-ion battery [8].

Various methods can be used so that lithium-ion batteries do not overheat using active and passive cooling methods. Active cooling works by utilizing external energy to run properly, with examples such as cooling fans or pumps to deliver coolant to the battery. Meanwhile, passive cooling has a working principle that does not require external energy, such as a heatsink that cools with the absorption of the heat generated and then discards it to the environment [9]. In this study, the cooling method used is active cooling by introducing cooling fluid flowing into the battery.

Liquid cooling has advantages in the cooling process compared to air cooling, such as being able to maintain lower temperatures and better temperature uniformity of the battery [10]. Liquid cooling is effective in preventing battery overheating due to its high heat capacity. The focus of this study is on cooling, which involves the circulation of a cooling fluid consisting of water and ethylene glycol through mini channels. Ethylene Glycol, a compound with no color or odor and low viscosity possesses thermal properties such as a high boiling point, low freezing point and stability across various temperatures. By incorporating ethylene glycol the boiling point of water can be raised while lowering its freezing point [11]. For this research a 50:50 mixture of ethylene glycol and water is utilized. The study aims to explore the impact of mass flow rate and the number of channels in the mini-channel cooling plate using different cooling fluids (water fluid and ethylene glycol) on temperature distribution, within lithium ion batteries.

2 Methodology

Simulations using Computational Fluid Dynamics (CFD) to analyze the cooling system of prismatic lithium-ion battery cells with mini-channel cooling plates are conducted. For this

study, CFD software of ANSYS Fluent 2019 R2 is utilized. Simulations adjusting variables like mass flow rate and the number of channels is performed. **Figure 2** illustrates the design of shaped lithium-ion batteries.

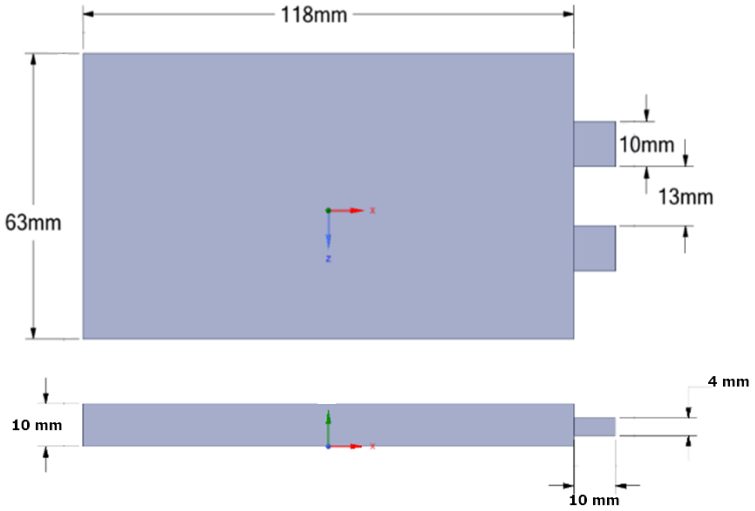

Fig. 2. Battery geometry design.

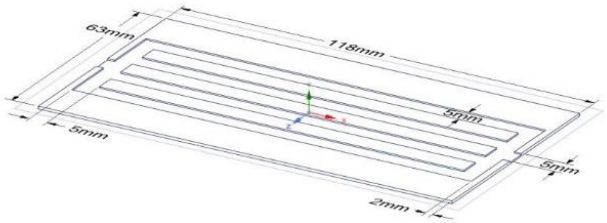

Fig. 3. Design of the cooling plate geometry.

The battery cooling plate, featuring a channel is illustrated in **Figure 3**. It has a thickness of 1 mm and a channel depth of 5 mm. The plate is made of aluminum. This plate is positioned adjacent to a lithium-ion battery. The number of channels can range from 4 to 5 each with a width of 5 mm. To cool the system, the cooling fluid enters through an inlet. Exits through an outlet situated on the opposite side of the cooling plate.

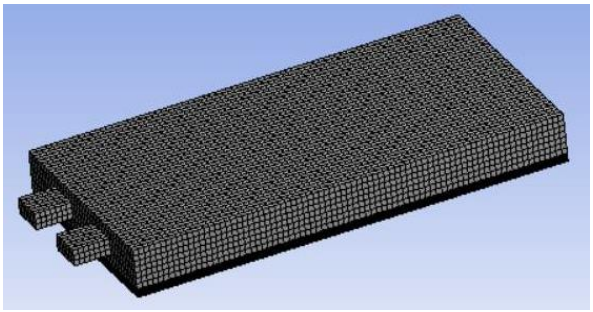

Fig. 4. Geometric meshing results

The minimum orthogonal mesh quality produced with the input of such parameters is 0.68725 and a maximum of 1. The quality of the meshing is still in the good range [12]. **Figure 4** shows the mesh result for the simulation domain.

The battery's heat generation comes from the heat produced by the reaction (Q_r) and current resistance (Q_j). To calculate the heat from the reaction you can use the formula;

$$Q_r = T\Delta S\frac{I}{n \times F} \quad (1)$$

where I is a discharge voltage (A), the process involves the movement of a number of electrons represented by the variable n, F is the Faraday constant (9,658.4 C·mole^{-1}), ΔS is an entropy change (Js^{-1} K^{-1}), and T is a temperature (K). The heat from current resistance can be calculated as follows

$$Q_j = I(E - V) \quad (2)$$

where the heat generated by the battery can be calculated by considering the open voltage circuit (E) and the operational voltage (V) which depend on temperature and state of charge (SOC) such that

$$Q_{gen} = I(E - V) + T\Delta S\frac{I}{n \times F} \quad (3)$$

Based on the tabulated data in Table 2, the heat generated by the battery is 7,232 W.

Table 2. Lithium-Ion Battery Specification [13-15].

Property	Value	Property	Value
ρ (Density)	2,500 kg/m^3	T (Operational temperature)	40°C
C_p (Specific Heat)	1,000 J/(Kg·K)	E (Open voltage circuit)	4.2 Volts
K (Thermal conductivity)	3 W/(m·K)	V (Operational voltage)	3.7 Volts
I (Battery Current)	26.5 A	ΔS (Entropy changes)	-35 J/(s·K)
Battery Capacity	5.6 Ah	n (Number of electron)	0.5

The properties of the cooling fluid and aluminum cooling plate utilized in this simulation are listed in Table 3 as shown below.

Table 3. Cooling fluid and aluminum cooling plate properties [16-18].

Property	50% Ethylene Glycol/50% Water	100% Water	Aluminium Cooling Plate
ρ (Density)	1,087 kg/m^3	998,2 kg/m^3	2,719 kg/m^3
C_p (Specific Heat)	3,285 J/(kg·K)	4,184 J/(Kg·K)	871 J/(Kg·K)
K (Thermal conductivity)	0.37 W/(m·K)	0.598 W/(m·K)	202.4 W/(m·K)

The other boundary condition and method used in this simulation is tabulated in Table 4 as follows:

Table 4. Boundary Conditions and Method.

Boundary Conditions/Methods	Setting
Types of analysis	*Transient*
Solver Type	*Pressure based*
Energy	*On*
Velocity Formulation	*Absolute*
Flow	*Laminar* (Re < 2,300)
Inlet	Temperature: 26.85°C Mass flow rate variation: 1×10^{-5} and 1×10^{-4} kg/s
Outlet	Type: *Outflow*
Wall battery and cooling	Type: Convection with h = 5 W/(m^2·K)

3 Results and Discussion

3.1 Mesh Independence Study

A mesh independence analysis is conducted by comparing the element count in the model with the temperature outlets obtained from the simulation process. The purpose of the mesh independence study is to be able to use the most optimal meshing for the simulation process so that the simulation process can run as lightly and optimally as possible. To some extent, the greater the number of elements used, the more accurate the modeling will be. The result of the mesh independence study and the percentage error are detailed in Table 5.

From Table 5, the number of elements of 5,385,501 has a relatively small error compared to others. **Figure 5** shows that simulation with the number of elements of 1,126,617 is comparably acceptable in terms of error and this smaller number of elements will help to reduce the computation time, thus, the number of elements of 1,126,617 is selected for this study.

Table 5. Results of mesh independence study

No	Element size (mm)	Number of *nodes*	Number of elements	$\%Error = \frac{T_{new}-T_{old}}{T_{old}}$
1	Battery 0.25 Cooler 0.75	5,662,073	5,385,501	4.13
2	Battery 0.5 Cooler 1	1,336,113	1,126,617	4.51
3	Battery 0.75 Cooler 1.25	899,044	761,228	5.43
4	Batterai 1 Cooler 1.5	778,828	649,133	6.22
5	Batterai 1.5 Cooler 2	720,722	597,019	6.71

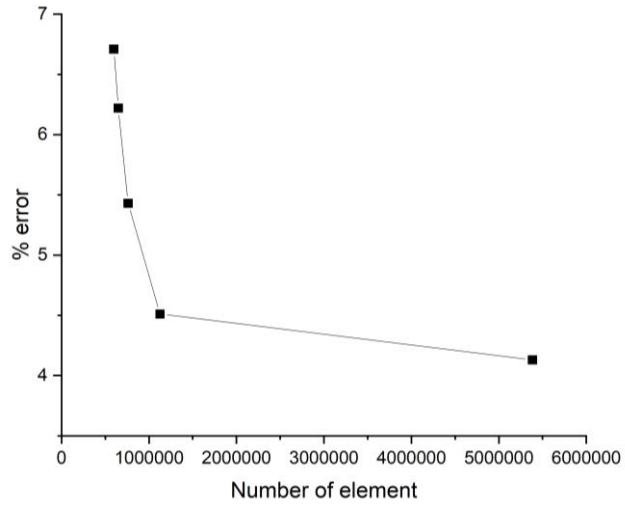

Fig. 5. Mesh independence study of lithium-ion battery

3.2 Effects of Mass Flow Rate

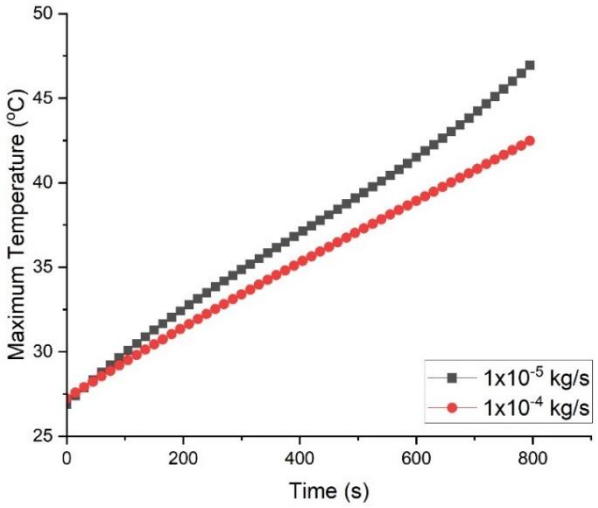

Fig. 6. Maximum temperature of lithium-ion battery with water cooling fluid at different mass flow rate

In this study when the prismatically shaped lithium-ion battery generated 7,232 W of heat, the surface of the battery was cooled by adjusting the flow rate of the cooling fluid. The absorbed heat from the battery is then carried away through a channel that runs from the inlet to the outlet. Lithium-ion batteries are quite sensitive to overheating. If left unchecked, it can impact the batterys quality and lifespan. In **Figure 6**, the temperature of a lithium-ion battery is observed when using water cooling fluid at different mass flow rates. The graph demonstrates that a higher mass flow rate of 1×10^{-4} kg/s results in a lower maximum temperature compared to a

mass flow rate of 1×10^{-5} kg/s. Similarly in **Figure 7**, the maximum temperature of a lithium-ion battery utilizing 50% ethylene glycol cooling fluid at different mass flow rates is shown. This result follows the same trend as water-cooling showing that higher mass flow rates lead to lower maximum temperatures.

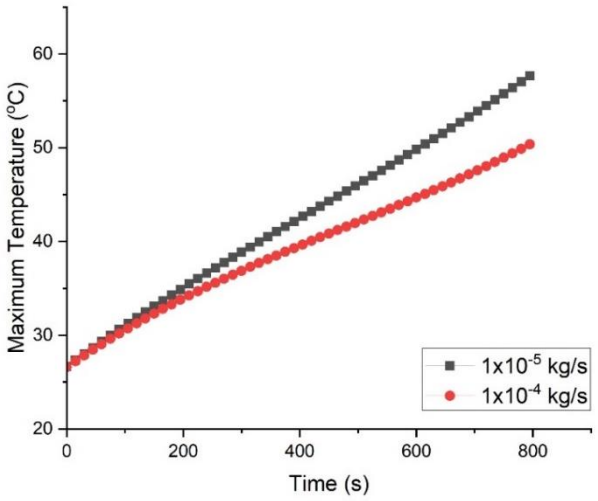

Fig. 7. Maximum temperature of lithium-ion battery with 50% ethylene glycol cooling fluid at different mass flow rate

Figure 8 show the contours of temperature at cooling plate of 5 mini channels with mass flow rate of 1×10^{-4} kg/s for water-cooling fluid and 50% ethylene glycol, and with mass flow rate of 1×10^{-5} kg/s for water-cooling fluid and 50% ethylene glycol. Based on the simulation results of the cooling plate it can be observed from **Figure 8**.**(a)** and **Figure 8**.**(b)** that a mass flow rate of 1×10^{-4} kg/s has an average temperature of 38°C. In contrast a mass flow rate of 1×10^{-5} kg/s shows a higher average temperature of 47°C as depicted in **Figure 8**.**(c)** and **Figure 8**.**(d)**. The velocity is higher for the mass flow rate of 1×10^{-4} kg/s at 0.04 m/s whereas it is only at 0.004 m/s for the mass flow rate of 1×10^{-5} kg/s. Higher velocity leads to a decrease in thermal boundary layer thickness or an increase in temperature gradient thus enhancing heat transfer. A similar pattern is observed in the temperature distribution at the lithium-ion battery as shown in **Figure 9** and at the cooling channel as shown in **Figure 10**. The cooling plate and cooling channel have a lower temperature range because they are responsible for dissipating the heat generated by the lithium-ion battery.

Although the targeted maximum operational temperature of 35°C is not fully achieved with a mass flow rate of 1×10^{-4} kg/s it can be concluded that this flow rate performs better compared to the one with a mass flow rate of 1×10^{-5} kg/s in reaching the desired temperature range. This finding aligns with studies indicating that increasing the mass flow rate reduces temperature [13,18]. Furthermore, those studies also suggest that as the flow rate increases further to some extent, the impact on cooling performance diminishes.

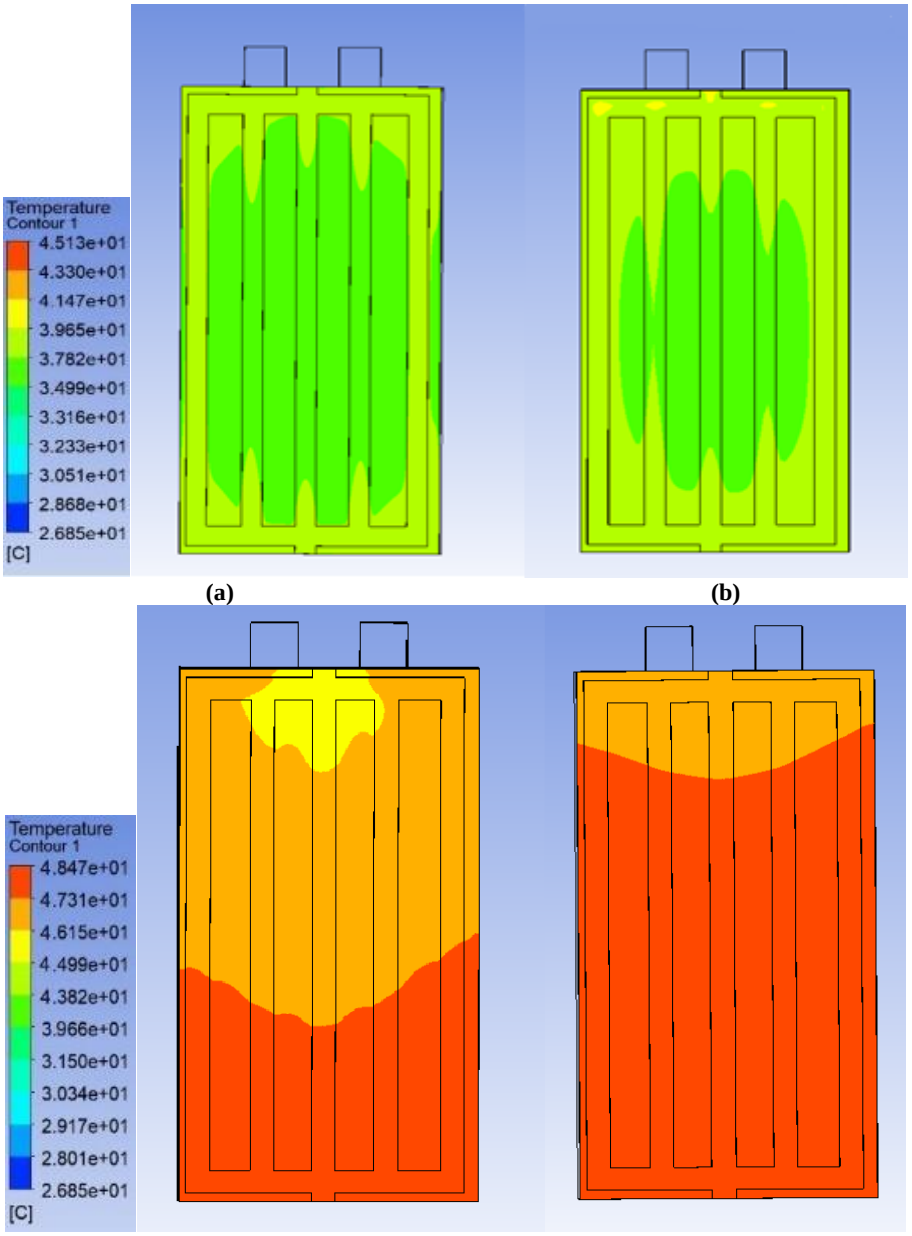

Fig. 8. Contours of temperature at cooling plate of 5 mini channels with mass flow rate of 1×10^{-4} kg/s for (a) water-cooling fluid and (b) 50% ethylene glycol, and with mass flow rate of 1×10^{-5} kg/s for (c) water-cooling fluid and (d) 50% ethylene glycol

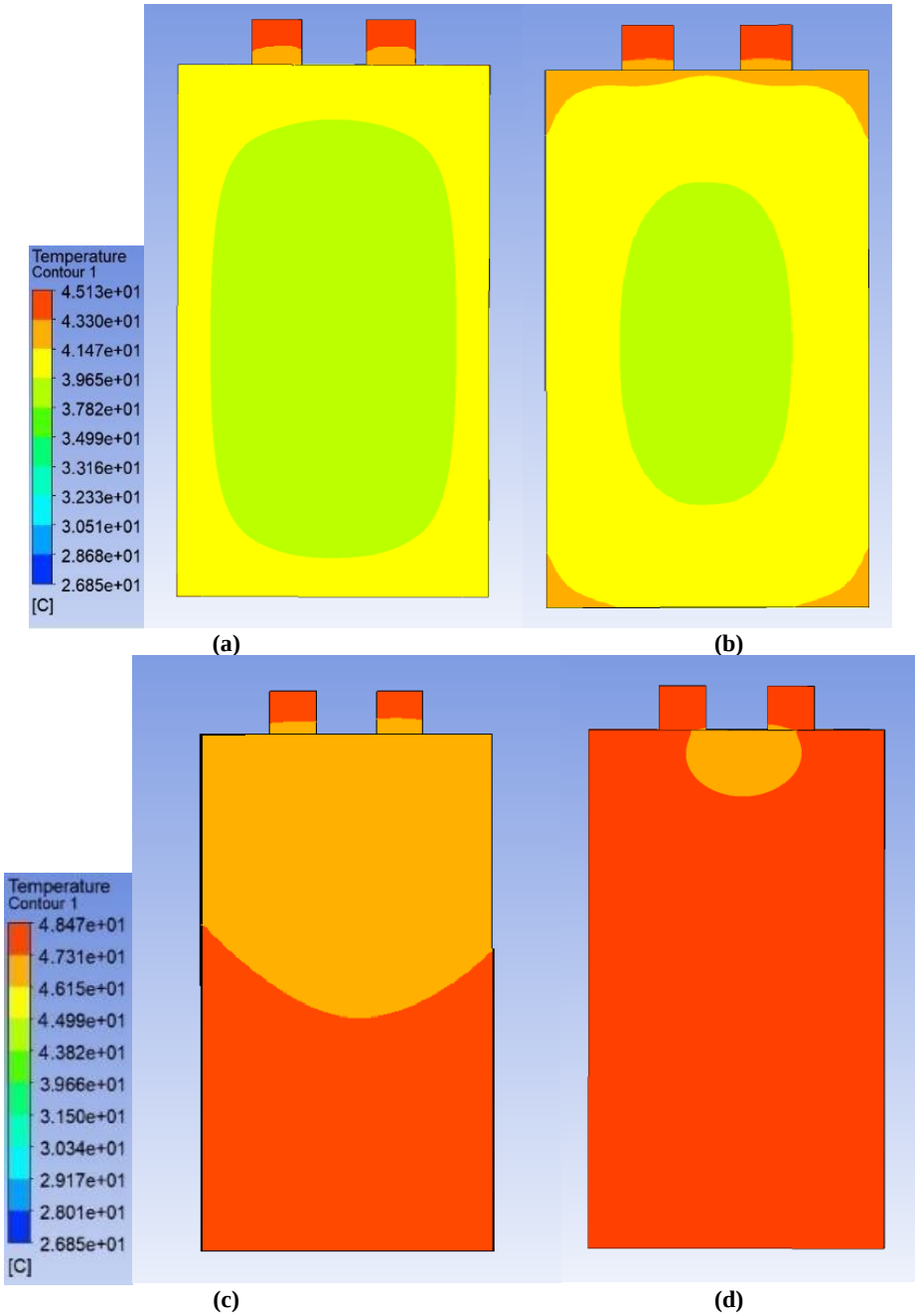

Fig. 9. Contours of temperature at lithium-ion battery of 5 mini channels with mass flow rate of 1×10^{-4} kg/s for (a) water-cooling fluid and (b) 50% ethylene glycol, and with mass flow rate of 1×10^{-5} kg/s for (c) water-cooling fluid and (d) 50% ethylene glycol

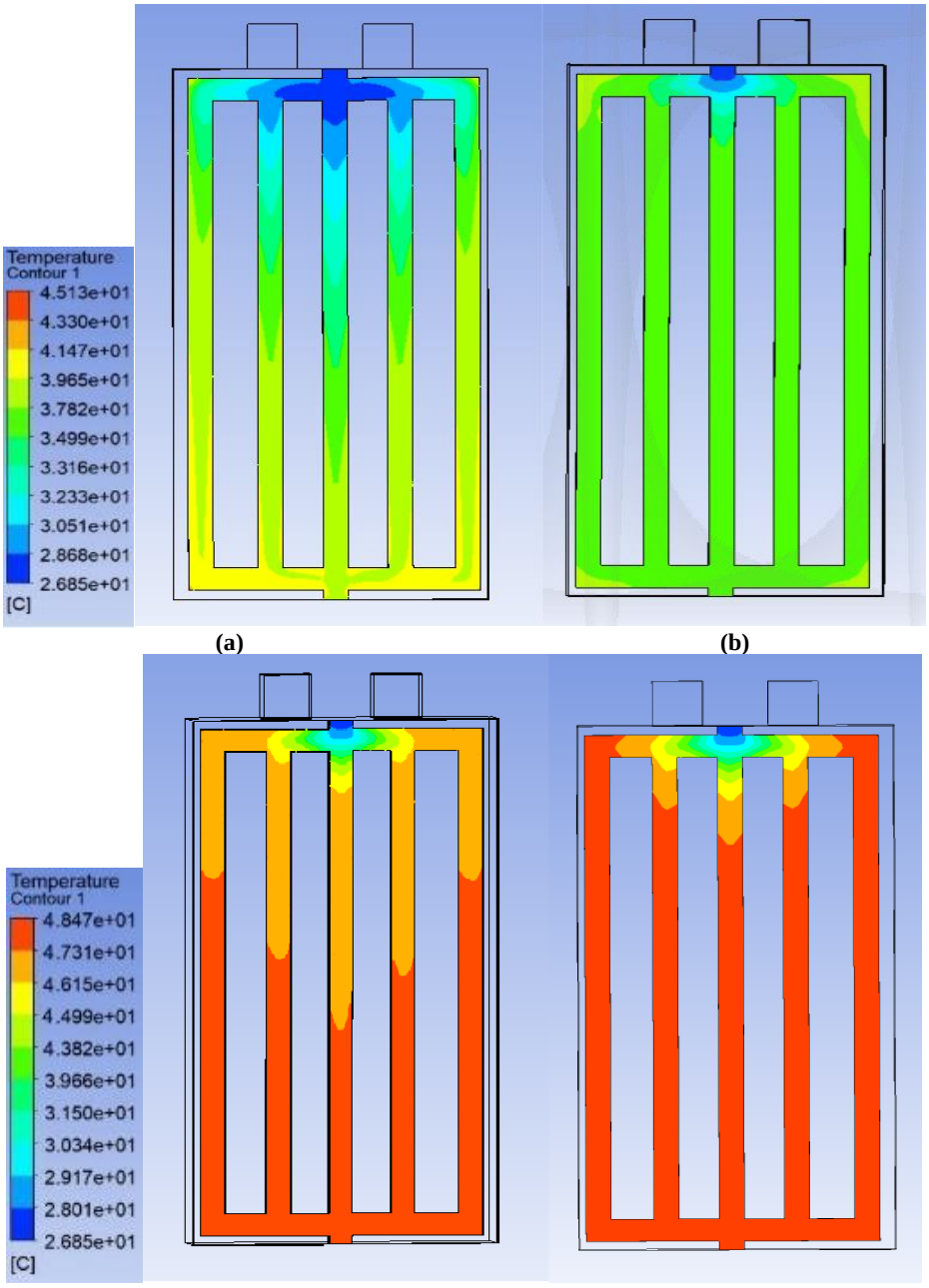

Fig. 10. Contours of temperature at cooling channel of 5 mini channels with mass flow rate of 1×10^{-4} kg/s for (a) water-cooling fluid and (b) 50% ethylene glycol, and with mass flow rate of 1×10^{-5} kg/s for (c) water-cooling fluid and (d) 50% ethylene glycol

The increased thermal efficiency observed for a mass flow rate of 1×10^{-4}kg/s is balanced with a pressure drop more than 11 times greater than that of a mass flow rate of 1×10^{-5}

kg/s as indicated in Table 6. This discrepancy arises due to the higher mass flow rate leading to increased velocity thus resulting in friction and losses within the bends of the channel. It is commonly observed that an improvement in performance is accompanied by an elevation in pressure drop.

Table 6. Comparison of pressure drop with different mass flow rate.

No.	Mass flow rate (kg/s)	Number of *channels* (mm)	*Pressure Drop* (Pa)
1	1×10^{-5}	5	5.8417
2	1×10^{-4}	5	66.23

3.3 Effects of Cooling Fluid

In **Figure 11**, the temperature of a lithium-ion battery over time using different cooling fluids of water and a 50% ethylene glycol solution. The figure clearly demonstrates that water, as a cooling fluid performs better in terms of cooling rate compared to the 50% ethylene glycol solution. The cooling fluid of water can reduce battery maximum temperature by 18.6% better than the cooling fluid of 50% ethylene glycol. This is because water has a higher heat capacity with a specific heat of 4,184 J/(Kg·K) compared to 50% ethylene glycol with a specific heat of 3285 J/(Kg·K). Water also has better temperature distribution due to a higher thermal conductivity of 0.598 W/(m·K) while 50% ethylene glycol has only thermal conductivity of 0.37 W/(m·K).

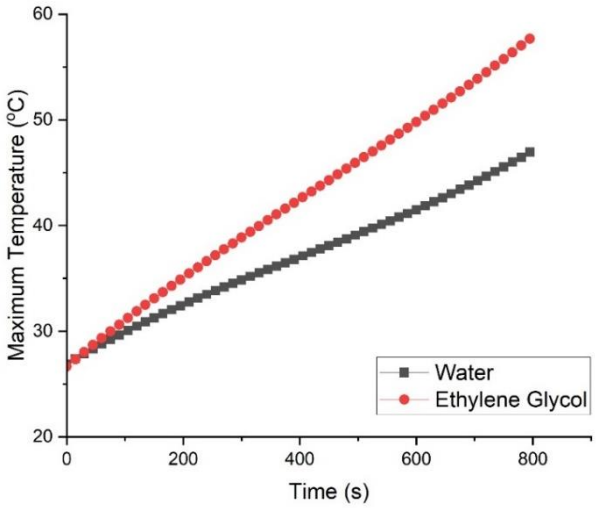

Fig. 11. Maximum temperature of lithium-ion battery with different cooling fluid of water and 50% ethylene glycol

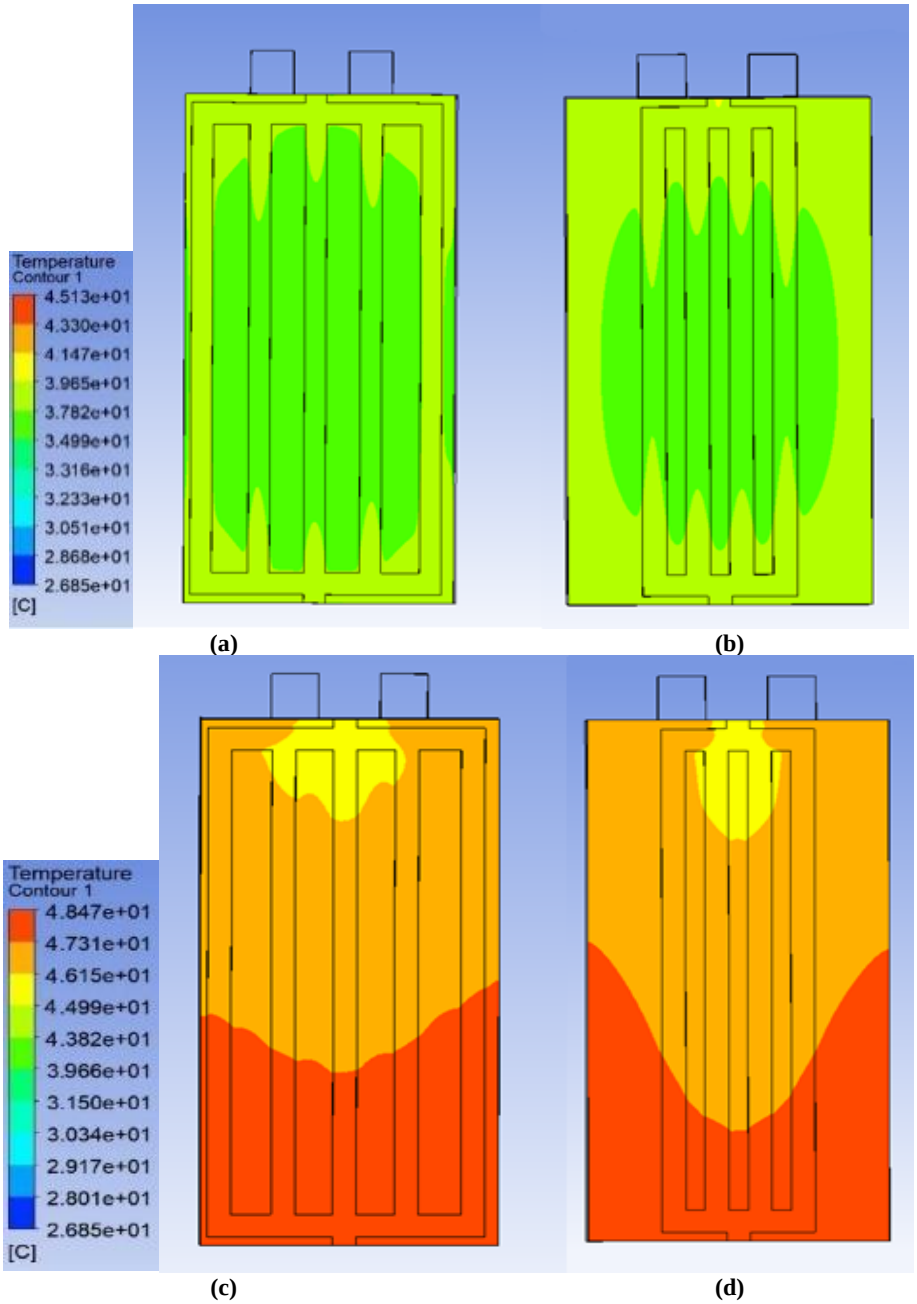

Fig. 12. Contours of temperature at the cooling plate of water-cooling fluid with mass flow rate of 1×10^{-4} kg/s for (a) 5 mini channels and (b) 4 mini channels, and 50% ethylene glycol with mass flow rate of 1×10^{-5} kg/s for (c) 5 mini channels and (d) 4 mini channels

3.4 Effects of Channels Number

In the study **Figure 12** illustrates the temperature contours at a cooling plate of water-cooling fluid with a mass flow rate of 1×10^{-4} kg/s for 5 and 4 mini channels, and 50% ethylene glycol with mass flow rate of 1×10^{-5} kg/s for 5 and 4 mini channels. It can be observed that increasing the number of channels only leads to a slight reduction in the average temperature range. This finding aligns with research that indicates a small increase in heat transfer rate or decrease in temperature as the number of channels increases [13,18]. More channels contribute to better temperature distribution and incorporating phase change material can further enhance this distribution compared to using single phase cooling material [19]. Table 7 presents the pressure drop results for numbers of channels. Notably the cooling plate, with four channels exhibits a lower pressure drop.

Table 7. Comparison of pressure drop with different number of channels.

No.	Mass flow rate (kg/s)	Number of *channels*	*Pressure Drop* (Pa)
1	1×10^{-5}	4	7.3021
2	1×10^{-5}	5	5.842

In addition, to factors like the mass flow rate, number of channels, and type of cooling fluid it is important to investigate the variation of the mini-channel and heating load ranges when designing a battery thermal management system. These elements proof to have influence on the performance of the cooling design [20,21].

4 Conclusions

A study was carried out to simulate the management of lithium-ion batteries. The study involved varying the mass flow rates of 1×10^{-4} kg/s and 1×10^{-5} kg/s as changing the number of channels from 4 to 5. Two types of cooling fluids water and a mixture of 50% ethylene glycol were also examined. Controlling the mass flow rate is crucial for maintaining an operating temperature. The desired maximum operating temperature in lithium-ion battery of 35°C should be able to achieve by giving mass flow rate of $> 1 \times 10^{-4}$kg/s for this specific case. By increasing the mass flow rate, it was observed that the maximum temperature in the battery could be reduced by up to 12.6%. However, this reduction came at a cost of more than 11 times increase in pressure drop. The study also compared the cooling performance between water and a mixture of 50% ethylene glycol. It was found that water performed better in terms of cooling efficiency. Additionally increasing the number of channels from four to five showed differences in temperature distribution but resulted in a significant reduction (up to 25%) in pressure drop. Overall, these findings highlight the importance of controlling mass flow rate and choosing cooling fluids for thermal management, in prismatic lithium-ion batteries.

References

[1] BPS – Statistics Indonesia, Number of Motor Vehicle by Type (Unit), 2018-2020, (2020)
[2] Kwade, A., Diekmann, J., Recycling of Lithium-Ion Batteries, Springer Cham, (2018)

[3] Megahed, S., Scrosati, B., Lithium-ion rechargeable batteries, Journal of Power Sources, vol. 51, no. 1–2, pp. 79-104, (1994)
[4] Jaguemont, J., Boulon, L., Dubé, Y., A comprehensive review of lithium-ion batteries used in hybrid and electric vehicles at cold temperatures, Applied Energy, vol. 164, pp. 99-114, (2016)
[5] Bizon, N. and Tabatabaei, N. M., Advances in Energy Research: Energy and Power Engineering, Nova Science Publishers Inc., USA, (2013)
[6] Chen, R., Battery Pack Design of Cylindrical Lithium-Ion Cells and Modelling of Prismatic Lithium-Ion Battery Based on Characterization Test, Master's Thesis McMaster University, (2022)
[7] Greco, A., Cao, D., Jiang, X., Yang, H., A theoretical and computational study of lithium-ion battery thermal management for electric vehicles using heat pipes, Journal of Power Sources, vol. 257, pp. 344-355, (2014)
[8] Smith, K., NREL milestone report, (2008)
[9] Pesaran, A., Battery Thermal Management in EVs and HEVs: Issues and Solutions. Battery Man, vol. 43, (2001).
[10] Akbarzadeh, M., Kalogiannis, T., Jaguemont, J., Jin, L., Behi, H., Karimi, D., Beheshti, H., Mierlo, J.V., Berecibar, M., A comparative study between air cooling and liquid cooling thermal management systems for a high-energy lithium-ion battery module, Applied Thermal Engineering, vol 198, (2021)
[11] Peyghambarzadeh, S.M., Hashemabadi, S.H., Hoseini, S.M., Jamnani, M.S., Experimental Study of Heat Transfer Enhancement Using Water/Ethylene Glycol Based Nanofluidsas a New Coolant for Car Radiators. Heat and Mass Transfer, vol. 38, no. 9, pp. 1283-1290. (2011)
[12] Ansys, Ansys 12 User Guide, (2009)
[13] Huo, Y., Rao, Z., Liu, X., & Zhao, J., Investigation of power battery thermal management by using mini-channel cold plate. Energy Conversion and Management, vol. 89, pp. 387–395, (2015)
[14] Yazami, R., Thermodynamics of Electrode Materials for Lithium-Ion Batteries. Lithium Ion Rechargeable Batteries, pp. 67–102, (2010)
[15] Cupid, D. M., Ziebert, C., Schuster, E., Seifert, H. J., Thermodynamics and phase diagrams for lithium ion batteries, Phase Equilibria : Materials for the Future, pp. 29-32, (2012)
[16] Mohapatra, S., An overview of liquid coolants for electronics cooling. Electronics Cooling, (2006)
[17] National Institute of Standards and Technology, NIST Chemistry WebBook, U.S. Secretary of Commerce United States of America, (2021)
[18] Qian, Z., Li, Y., & Rao, Z., Thermal performance of lithium-ion battery thermal management system by using mini-channel cooling, Energy Conversion and Management, vol. 126, pp. 622–631, (2016)
[19] Rao, Z., Wang, S., Zhang, G., Simulation and experiment of thermal energy management with phase change material for ageing LiFePO4 power battery, Energy Conversion and Management, vol. 52, pp. 3408–3414, (2011).
[20] Liu, H., Gao, X., Niu, D., Yu, M., & Ji, Y., Thermal-Hydraulic Characteristics of the Liquid-Based Battery Thermal Management System with Intersected Serpentine Channels. Water, 14(19), 3148, (2022).
[21] Panchal, S., Gudlanarva, K., Tran, M.-K., Herdem, M. S., Panchal, K., Fraser, R., & Fowler, M., Numerical Simulation of Cooling Plate Using K-Epsilon Turbulence Model to Cool Down Large-Sized Graphite/LiFePO4 Battery at High C-Rates. World Electric Vehicle Journal, 13(8), 138, (2022).